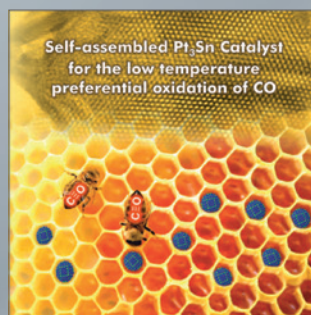
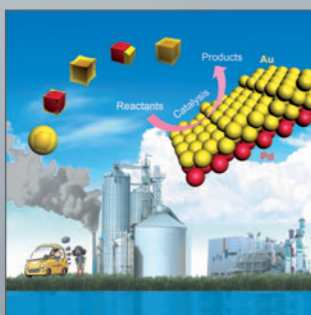
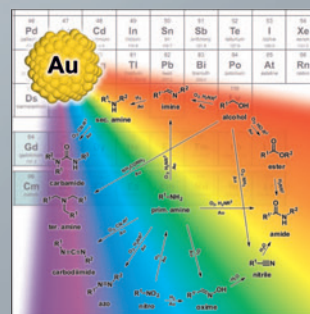
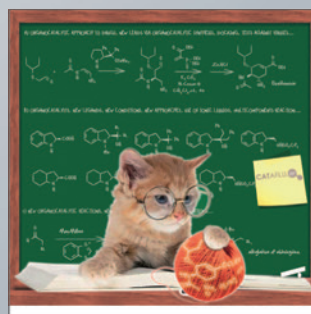
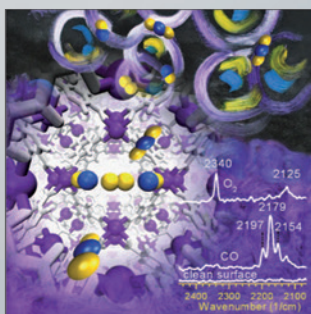
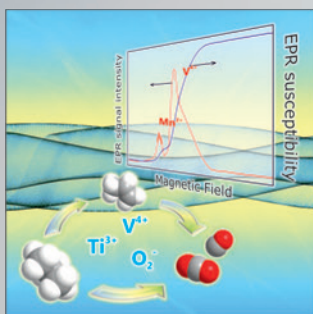
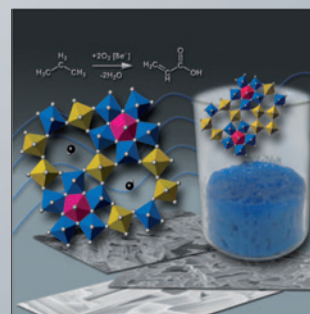
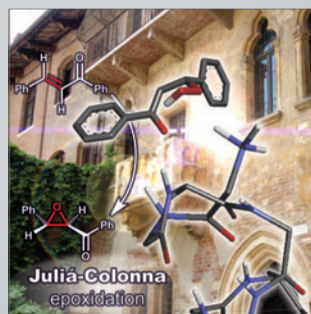
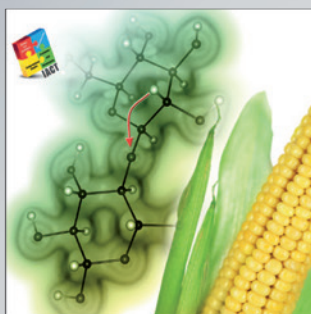
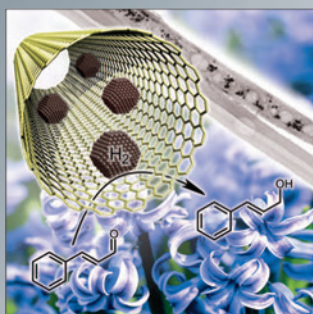


# Heterogeneous & Homogeneous & Bio- CHEMCATCHEM

## CATALYSIS



# Reprint

© Wiley-VCH Verlag GmbH & Co. KGaA, Weinheim

WILEY-VCH

[www.chemcatchem.org](http://www.chemcatchem.org)

A Journal of



# Cost-Effective Palladium-Doped Cu Bimetallic Materials to Tune Selectivity and Activity by using Doped Atom Ensembles as Active Sites for Efficient Removal of Acetylene from Ethylene

Riguang Zhang,<sup>[a, b]</sup> Bo Zhao,<sup>[a]</sup> Lixia Ling,<sup>[c]</sup> Anjie Wang,<sup>[d]</sup> Christopher K. Russell,<sup>[e]</sup> Baojun Wang,<sup>\*[a]</sup> and Maohong Fan<sup>\*[b, f]</sup>

The catalytic activity and selectivity of cost-effective noble-metal-doped common metal materials strongly depend on the doped atom ensemble in specific arrangements to provide active sites. In this study, aiming at insight into the doped atom ensembles as active sites for tuning the selectivity and activity towards the target reaction, different doped noble metal Pd atom ensembles for cost-effective Pd-doped Cu catalysts act as active sites to investigate the activity and selectivity towards the efficient removal of acetylene from ethylene by using density functional theory calculations. The results show that an ensemble composed of one surface and its joint sub-

layer Pd atoms in the Cu catalyst as active sites enhance both the selectivity and activity of  $C_2H_4$  formation caused by adjusting the catalyst surface electronic structure. Moreover, the surface d-band center of the Pd-doped Cu catalyst can act as an effective “descriptor” for the rapid screening of catalytic activity in the design of improved catalysts with the noble-metal-doped common metal. Further, the ensemble composed of one surface and its joint sublayer doped Pd atoms as active sites in the cost-effective Pd-doped Cu bimetallic catalysts is an efficient approach to finely tune the activity and selectivity towards the efficient removal of acetylene from ethylene.

## 1. Introduction

In heterogeneous catalysis, cost-effective noble-metal-doped common metal materials have been widely used, in which the “ensemble effect” with a very limited number of noble atoms often acts as active site, and usually plays an essential role in catalytic reactions.<sup>[1–3]</sup> Especially, the catalytic activity and selectivity of bimetallic catalysts with a small amount of noble metal in the common elements strongly depend on “ensemble effects” that describe the synergistic behavior of different constituents in specific arrangements.<sup>[2,4]</sup> Thus, identifying the structure and nature of such ensembles as active sites is an ef-

fective approach to understand and enhance the catalytic performance of bimetallic catalysts.<sup>[5–10]</sup>

Nowadays, cost-effective noble metal Pd-doped Cu bimetallic catalysts have started to be applied in the efficient removal of acetylene from ethylene by  $C_2H_2$  hydrogenation to  $C_2H_4$ ,<sup>[11–15]</sup> in this catalytic reaction,  $C_2H_2$  wastes that degrade the Ziegler–Natta catalysts for  $C_2H_4$  polymerization are converted into industrial feed stock  $C_2H_4$ . Even doping a very small quantity of noble-metal Pd into a Cu catalyst can exhibit a higher activity and selectivity towards  $C_2H_2$  hydrogenation to

[a] Prof. Dr. R. Zhang, Dr. B. Zhao, Prof. Dr. B. Wang  
Key Laboratory of Coal Science and Technology of Ministry of Education and Shanxi Province  
Taiyuan University of Technology  
Taiyuan 030024, Shanxi (P.R. China)  
E-mail: wangbaojun@tyut.edu.cn

[b] Prof. Dr. R. Zhang, Prof. Dr. M. Fan  
Department of Chemical Engineering and Department of Petroleum Engineering  
University of Wyoming  
Laramie, WY 82071 (USA)  
E-mail: mfan@uwyo.edu

[c] Prof. Dr. L. Ling  
College of Chemistry and Chemical Engineering  
Taiyuan University of Technology  
Taiyuan 030024, Shanxi (P.R. China)

[d] Prof. Dr. A. Wang  
State Key Laboratory of Fine Chemicals  
School of Chemical Engineering

Dalian University of Technology  
Dalian 116024, Liaoning (P.R. China)

[e] Dr. C. K. Russell  
Department of Civil and Environmental Engineering  
Stanford University  
Stanford, CA 94305 (USA)

[f] Prof. Dr. M. Fan  
School of Civil and Environmental Engineering  
Georgia Institute of Technology  
Atlanta, GA 30332 (USA)

Supporting information for this article can be found under: <https://doi.org/10.1002/cctc.201701899>. The Supporting Information includes the details of the calculation method of Gibbs free energy (Part 1), two-step model and the adsorption free energy barrier (Part 2), the most stable adsorption configurations of  $C_2H_x$  ( $x=2-5$ ) and H species on different Pd-doped Cu surfaces (Part 3), the structures of initial states, transition states, and final states of all elementary reactions involving in the selective hydrogenation of  $C_2H_2$  over different Pd-doped Cu surfaces (Part 4), the surface d-band center (Part 5), formation energy (Part 6), and the formation of 1,3 butadiene on a Cu(111) surface (Part 7).

C<sub>2</sub>H<sub>4</sub> than the pure Cu or Pd alone.<sup>[1,14,15]</sup> For Pd-doped Cu bimetallic catalysts, one arrangement leading to an “ensemble effect” that has attracted attention is an ensemble of surface Pd atoms acting as active sites,<sup>[1]</sup> the other is an ensemble composed of surface and sublayer Pd atoms acting as active sites.<sup>[3,14,16,17]</sup>

Although demonstrated experimentally,<sup>[1,14,15]</sup> the theoretical understanding of this catalytic reaction is lacking, and the actual structure and nature of active sites in Pd-doped Cu bimetallic catalysts catalyzing C<sub>2</sub>H<sub>2</sub> hydrogenation, whether as a result of an ensemble of surface Pd atoms as active sites or an ensemble composed of surface and sublayer Pd atoms as active sites, still remains unclear. Further, the ensemble effect on the activity and selectivity towards C<sub>2</sub>H<sub>4</sub> formation is also unknown. Up to now, it is still difficult to elucidate the structure and nature of the active site(s) and the ensemble roles by using experiments alone. Fortunately, calculations using density functional theory (DFT) can be used to understand the details of catalytic phenomena, the structure and nature of active sites, the ensemble role of atomic arrangement, and the mechanistic details. Such detailed knowledge can be used to design catalysts with superior performance and specific experiments to better understand mechanistic details.<sup>[18–25]</sup>

This study was designed to make progress in understanding the catalytic performances of the cost-effective Pd-doped Cu bimetallic catalysts towards efficient removal of acetylene from ethylene, and gain insight into the effects of doped noble-metal atom ensembles as active sites on the catalytic activity and selectivity by using density functional theory (DFT) calculations. Here, different types of doped Pd atom ensembles as active sites, including the ensemble of surface Pd atoms and the ensemble composed of surface–sublayer Pd atom configurations, are considered. The results not only find the ensemble arrangements that are most suitable to enhance the activity and selectivity of active sites towards C<sub>2</sub>H<sub>4</sub> formation over Pd-doped Cu bimetallic catalysts, but also provide an efficient approach to tune the selectivity and activity of cost-effective bimetallic catalysts using a very limited quantity of noble-metal atoms doped into the common elements in industrially key hydrogenation reactions.

## 2. Computational Details

### 2.1. Computational method

DFT calculations were performed by using the Dmol<sup>3</sup> program package in Materials Studio 5.5,<sup>[26,27]</sup> the generalized gradient approximation (GGA) with the exchange–correlation functional PBE proposed by Perdew–Burke–Ernzerhof<sup>[28,29]</sup> was employed. In the computation,  $2.0 \times 10^{-5}$  Ha,  $4.0 \times 10^{-3}$  Ha Å<sup>-1</sup>, and  $5.0 \times 10^{-3}$  Å were set for the energy convergence, maximum force, and maximum distance. To expand the valence electron function, the double numerical basis set with a polarization d-function (DNP) was selected.<sup>[30]</sup> A  $3 \times 3 \times 1$  *k*-point sampling in the surface Brillouin zone was used for analyzing Cu(111) and Pd-doped Cu surfaces. The orbital cutoff range was set as medium quality, and 0.005 Hartree was set for the smearing value. An

effective core potential (ECP) is used for Cu and Pd atoms and all-electron basis sets for other atoms.

To obtain accurate activation barriers of elementary reactions involved in the selective hydrogenation of C<sub>2</sub>H<sub>2</sub>, the transition state (TS) of every elementary reaction was searched by using the complete LST (linear synchronous transit)/QST (quadratic synchronous transit) method.<sup>[31,32]</sup> All transition states were confirmed by ensuring only one imaginary frequency, and by using TS confirmation to show that the transition state is connected with the reactant and product.

Oligomerization of C<sub>2</sub>H<sub>2</sub> can be effectively inhibited by high H<sub>2</sub>/C<sub>2</sub>H<sub>2</sub> ratios and high temperatures, reducing the formation of “green oil”,<sup>[4,15,33,34]</sup> so a high temperature of 425 K used in experiments is considered. Contributions of zero-point vibrational energy (ZPE), thermal energy, and entropy to the molar Gibbs free energy have been included. The entropies of gaseous H<sub>2</sub>, C<sub>2</sub>H<sub>2</sub>, and C<sub>2</sub>H<sub>4</sub> species under standard conditions are taken from experimental databases, and are used for calculating the entropies at 425 K. The total pressure is set to 1.0 atm along with an H<sub>2</sub>/C<sub>2</sub>H<sub>2</sub> ratio of 10:1, leading to partial pressures of H<sub>2</sub>, C<sub>2</sub>H<sub>2</sub>, and C<sub>2</sub>H<sub>4</sub> of 0.1, 0.01, and 0.89 atm, respectively, similar to experimental conditions used for comparison.<sup>[33]</sup>

Further, it is found that the Pd-based catalysts during the C<sub>2</sub>H<sub>2</sub> hydrogenation reaction can form Pd hydride and Pd carbide owing to the formation of subsurface species like C and H species, which can affect the selectivity of C<sub>2</sub>H<sub>2</sub> hydrogenation.<sup>[33,35–37]</sup> Hu et al. have proved that the subsurface H atoms on the Pd catalyst can improve the selectivity of ethylene more than the pure Pd catalysts.<sup>[38]</sup> However, for CuPd catalysts, recent works from Gapipaud et al.<sup>[39]</sup> and Friedrich et al.<sup>[40]</sup> suggest that CuPd mixtures do not form a hydride phase for Cu/Pd bulk ratios of 0.5 and above. Interestingly, Anderson et al.<sup>[15]</sup> by using temperature-programmed reduction (TPR) measurements found that on CuPd catalysts, there is no Pd-hydride for the CuPd ratios 100:1, 50:1, 25:1, and 10:1. Thus, the formation of Pd-hydride is difficult on CuPd catalysts, and the effect of Pd-hydride formation on the hydrogenation of C<sub>2</sub>H<sub>2</sub> is not considered in this study. Detailed descriptions of the calculations of Gibbs free energies of gaseous and adsorbed species, and the reactions are presented in the Part 1 of the Supporting Information.

### 2.2. Surface model

For the Cu catalyst, the (111) surface is the most stable and has the most dominantly exposed crystal facets with the lowest surface energy,<sup>[41–43]</sup> so it is generally chosen as the representative surface for experimental and theoretical studies.<sup>[3,14,41–43]</sup> Cu(111) is cleaved from the bulk with the lattice constant of 3.615 Å, and it is modeled by a four-layer  $p(3 \times 3)$  periodic slab with nine atoms in each layer (Figure 1(a)). The vacuum gap is set to 15 Å to separate the slabs, which is large enough to avoid interactions between the slabs.

To probe the ensemble effect of surface Pd atoms as the sites controlling the activity and selectivity in the selective hydrogenation of C<sub>2</sub>H<sub>2</sub> over Pd-doped Cu bimetallic catalysts, Cu atoms on the outmost layer are replaced by Pd atoms to con-

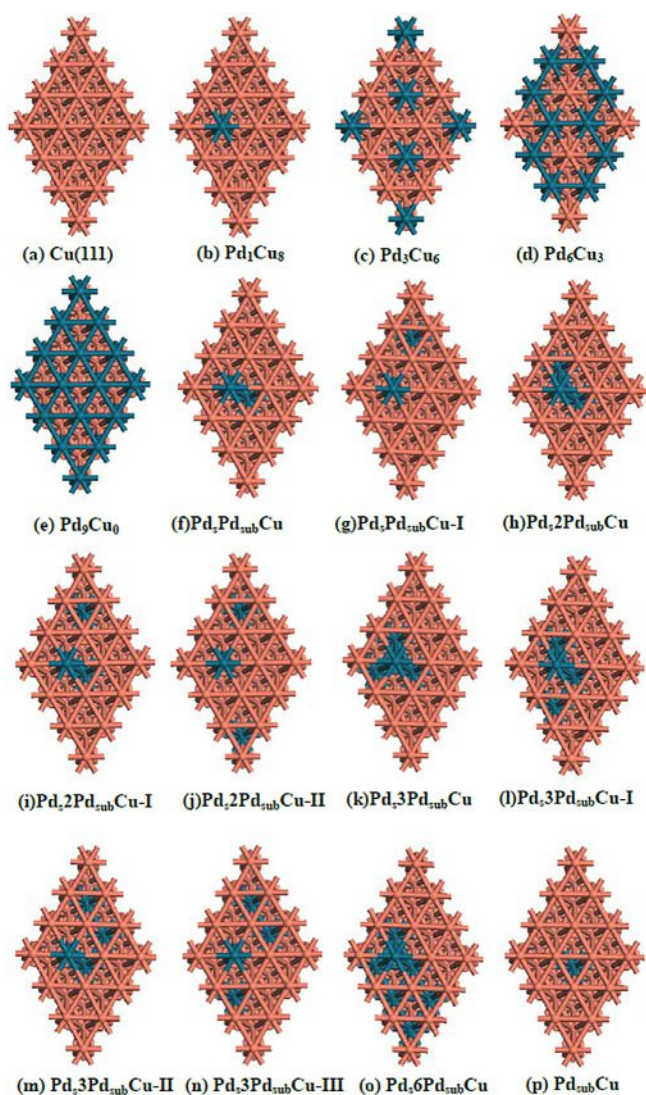


**Figure 1.** Surface structures with the different distributions of surface and sublayer Pd ensembles incorporated into a Cu surface.

struct PdCu bimetallic surfaces with different Pd geometrical distributions (Figure 1(b)–(e)). The nearest-neighbor arrangement is not considered as such a pattern has been firmly excluded by the experiments,<sup>[14]</sup> so four PdCu(111) surface configurations are likely, that is, six, three, and one outmost layer Cu atoms on the Cu(111) surface replaced by Pd atoms, which are named as Pd<sub>6</sub>Cu<sub>3</sub>, Pd<sub>3</sub>Cu<sub>6</sub>, and Pd<sub>1</sub>Cu<sub>8</sub>, respectively. Meanwhile, all nine outmost layer Cu atoms on Cu(111) replaced by Pd atoms is also considered, and denoted as Pd<sub>9</sub>Cu<sub>0</sub>. In addition, it should be noted that the Pd-Cu-Cu trimer ensemble appears on the Pd<sub>1</sub>Cu<sub>8</sub> and Pd<sub>3</sub>Cu<sub>6</sub> surfaces, and the Pd-Cu dimer ensemble appears on the Pd<sub>6</sub>Cu<sub>3</sub> surface, which can also present the effect of Pd-Cu-Cu trimer and Pd-Cu dimer ensembles on the formation of ethylene.

A specific aim of the calculations is to examine the ensemble when surface and sublayer Pd atoms interact to create active sites that drive the activity and selectivity in C<sub>2</sub>H<sub>2</sub> hydrogenation. As such, a series of PdCu bimetallic surfaces involving both the surface and sublayer Pd atoms are studied (Fig-

ure 1(f)–(o)), all surface-sublayer Pd-doped Cu catalysts are based on the Pd<sub>1</sub>Cu<sub>8</sub> surface, which is found to have the highest selectivity towards C<sub>2</sub>H<sub>4</sub> formation in the results presented below.

Cu atoms in the sublayer of Pd<sub>1</sub>Cu<sub>8</sub> are replaced with Pd atoms to construct PdCu bimetallic surfaces with different sublayer Pd geometrical distributions, which leads to different connection modes between one surface Pd atom and the sublayer Pd atoms. In addition, the case of a Pd<sub>sub</sub>Cu surface with one Cu atom in the sublayer replaced by one Pd atom is also considered (Figure 1(p)).

During the calculations, the top two layers of the PdCu bimetallic surfaces together with the adsorbed gaseous species were allowed to relax, whereas the bottom two layers were fixed at their bulk structure, resembling the unperturbed bulk atoms.

### 3. Results and Discussion

#### 3.1. Proposed mechanism for the selective hydrogenation of C<sub>2</sub>H<sub>2</sub>

For the selective hydrogenation of C<sub>2</sub>H<sub>2</sub>, two key factors affect the selectivity of C<sub>2</sub>H<sub>4</sub> formation: one is the over-hydrogenation of C<sub>2</sub>H<sub>2</sub> to ethane; the other is the formation of “green oil” through the polymerization of C<sub>2</sub>H<sub>2</sub>.<sup>[15,33,34]</sup> Previous experiments have shown that when the temperature is 425 K, and the H<sub>2</sub>/C<sub>2</sub>H<sub>2</sub> ratio is high,<sup>[15]</sup> the formation of “green oil” can be inhibited. Introducing Pd into the Cu(111) surface decreases the activation barrier of H<sub>2</sub> dissociation to 0.29 eV from the range 0.45–0.50 eV on the Cu(111) surface.<sup>[3]</sup> To focus this study specifically on C<sub>2</sub>H<sub>2</sub> over-hydrogenation to ethane, the temperature is set to 425 K and the H<sub>2</sub>/C<sub>2</sub>H<sub>2</sub> ratio is set to 10:1.

Three potential pathways are examined to determine the optimal pathway in the selective hydrogenation of C<sub>2</sub>H<sub>2</sub>,<sup>[33]</sup> as shown in Figure 2, the first path, the C<sub>2</sub>H<sub>4</sub> desorption pathway, is that C<sub>2</sub>H<sub>4</sub> is formed via the C<sub>2</sub>H<sub>3</sub> intermediate; C<sub>2</sub>H<sub>4</sub> then readily desorbs from the catalyst surface instead of being hydrogenated to ethane. The latter two paths are the over-hydrogenation of C<sub>2</sub>H<sub>2</sub> via C<sub>2</sub>H<sub>4</sub> or CH<sub>3</sub>CH intermediates to form C<sub>2</sub>H<sub>5</sub>, followed by its hydrogenation to ethane, which are denoted as the C<sub>2</sub>H<sub>4</sub> and CH<sub>3</sub>CH intermediate pathways, respectively. Thus, when the C<sub>2</sub>H<sub>4</sub> desorption pathway is the preferred pathway, the corresponding catalyst exhibits a better se-

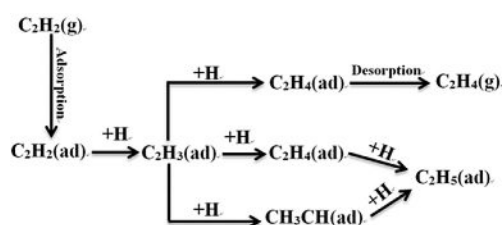


**Figure 2.** Three possible reaction pathways involved in the selective hydrogenation of C<sub>2</sub>H<sub>2</sub> via C<sub>2</sub>H<sub>4</sub> desorption pathway, as well as CH<sub>3</sub>CH and C<sub>2</sub>H<sub>4</sub> intermediate pathways, respectively; (ad) and (g) stand for the adsorbed and gas-phase states, respectively.

lectivity towards  $C_2H_4$  formation. If either the  $C_2H_4$  or  $CH_3CH_3$  intermediate pathways is the preferred pathway, the primary product of  $C_2H_2$  hydrogenation is ethane, and the catalyst will have a poor selectivity towards  $C_2H_4$  formation.

### 3.2. Adsorption of $C_2H_x$ ( $x=2-5$ ) and H species

The adsorption of  $C_2H_x$  ( $x=2-5$ ) and H species in the selective hydrogenation of  $C_2H_2$  on Cu(111) and Pd-doped Cu surfaces is examined explicitly as a potentially important set of reaction pathways.<sup>[44,45]</sup> The most stable adsorption configurations of these species are presented in Figures S3–S5 (in the Supporting Information) and the adsorption free energies at 425 K are listed in Table 1.

**Table 1.** The adsorption free energies of H and  $C_2H_x$  ( $x=2-5$ ) species involved in the selective hydrogenation of  $C_2H_2$  over different Pd-doped Cu surfaces at 425 K.

Surfaces	Adsorption free energy [kJ mol <sup>-1</sup> ]					
	H	$C_2H_2$	$C_2H_3$	$C_2H_4$	$CH_3CH$	$C_2H_5$
Cu(111)	240.7	147.0	201.2	68.1	292.8	111.3
Pd <sub>1</sub> Cu <sub>8</sub>	243.1	156.5	196.7	89.5	303.6	131.6
Pd <sub>3</sub> Cu <sub>6</sub>	233.6	144.4	201.6	86.1	288.9	132.4
Pd <sub>5</sub> Cu <sub>3</sub>	231.4	136.2	206.9	79.8	323.4	132.3
Pd <sub>9</sub> Cu <sub>0</sub>	237.0	141.9	228.8	92.8	370.5	147.0
Pd <sub>1</sub> Pd <sub>sub</sub> Cu	246.5	155.5	225.7	100.7	312.6	145.0
Pd <sub>2</sub> Pd <sub>sub</sub> Cu-I	244.7	160.8	216.0	92.9	316.3	129.3
Pd <sub>2</sub> Pd <sub>sub</sub> Cu-II	247.6	162.6	214.4	108.0	316.3	153.1
Pd <sub>2</sub> Pd <sub>sub</sub> Cu-III	249.2	164.1	232.5	103.6	317.4	137.8
Pd <sub>2</sub> Pd <sub>sub</sub> Cu-IV	246.8	167.5	218.9	105.3	303.6	139.3
Pd <sub>3</sub> Pd <sub>sub</sub> Cu	244.3	165.8	209.3	103.7	318.5	149.4
Pd <sub>3</sub> Pd <sub>sub</sub> Cu-I	224.3	162.0	216.7	106.5	312.1	139.2
Pd <sub>3</sub> Pd <sub>sub</sub> Cu-II	249.8	167.8	217.9	98.2	314.0	129.4
Pd <sub>3</sub> Pd <sub>sub</sub> Cu-III	236.9	163.4	203.8	83.2	301.9	122.3
Pd <sub>6</sub> Pd <sub>sub</sub>	244.7	168.6	215.5	115.4	330.6	152.3
Pd <sub>sub</sub> Cu	240.6	145.7	201.0	63.8	294.8	114.8

The feed gas in the  $C_2H_2$  process typically contains 0.1–1%  $C_2H_2$  and 89%  $C_2H_4$ .<sup>[33]</sup> Thus, only when the adsorption ability of  $C_2H_2$  is much stronger than that of  $C_2H_4$ , one can realize the removal of trace amounts of  $C_2H_2$  from a large amount of  $C_2H_4$ . In addition, it is noted that besides the hydrogenation reaction of  $C_2H_2$  to  $C_2H_4$  for the removal of trace amounts of  $C_2H_2$  from a large amount of  $C_2H_4$ , the adsorbent-based separation of  $C_2H_2$  from  $C_2H_4$  has also been well demonstrated as an energy- and cost-efficient strategy,<sup>[46,47]</sup> which is not considered in this study.

The results show that the adsorption ability of  $C_2H_2$  on Pd-doped Cu surfaces is much stronger than that of  $C_2H_4$ , which favors the adsorption, activation, and hydrogenation of trace  $C_2H_2$ . Further, the adsorption free energy of  $C_2H_4$  on the Pd-doped Cu surface is higher than that on the Cu(111) surface, inhibiting  $C_2H_4$  desorption, which can contribute to the Pd-based catalyst having a lower selectivity towards  $C_2H_4$  formation.

### 3.3. $C_2H_2$ hydrogenation on Cu(111) and Pd-doped Cu(111) surfaces

#### 3.3.1. $C_2H_2$ hydrogenation on the Cu(111) surface

As shown in Figure 3,  $C_2H_2$  hydrogenation to  $C_2H_3$  via transition state TS1-1 is exothermic (6.1 kJ mol<sup>-1</sup>) with an activation free energy of 121.6 kJ mol<sup>-1</sup>. This is lower than the adsorption free energy of  $C_2H_2$  (147.0 kJ mol<sup>-1</sup>), suggesting that  $C_2H_2$  hydroge-

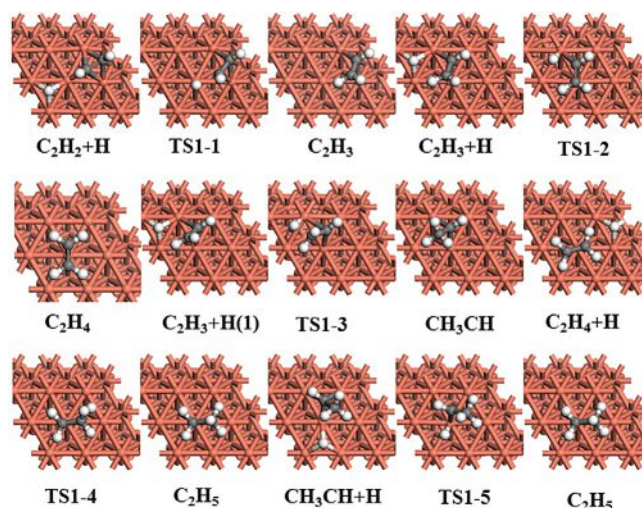


**Figure 3.** Free energy profiles of three pathways involved in the selective hydrogenation of  $C_2H_2$  on a Cu(111) surface together with the structures of initial states (ISs), transition states (TSs), and final states (FSs).

nation is more favorable than its desorption.  $C_2H_3$  hydrogenation to  $C_2H_4$  via TS1-2 has an activation free energy of 78.1 kJ mol<sup>-1</sup>, and is exothermic by 76.7 kJ mol<sup>-1</sup>; then,  $C_2H_4$  desorption from the surface has a free energy of 68.1 kJ mol<sup>-1</sup>.  $C_2H_4$  hydrogenation to  $C_2H_5$  via TS1-4 has the activation and reaction free energies of 81.1 and  $-17.0$  kJ mol<sup>-1</sup>, respectively.

Alternatively,  $C_2H_3$  hydrogenation to  $C_2H_5$  via the  $CH_3CH$  intermediate has the activation free energies of 101.4 and 61.5 kJ mol<sup>-1</sup> via TS1-3 and TS1-5 with the reaction energies of  $-12.3$  and  $-81.4$  kJ mol<sup>-1</sup>, respectively. The activation free energies of  $C_2H_3$  hydrogenation to  $C_2H_4$  and  $CH_3CH$  (78.1 and 101.4 kJ mol<sup>-1</sup>) are much lower than the adsorption free energy of  $C_2H_3$  (201.2 kJ mol<sup>-1</sup>), suggesting that  $C_2H_3$  hydrogenation can proceed without its desorption.  $CH_3CH$  hydrogenation is more favorable than its desorption as the activation free energy of  $CH_3CH$  hydrogenation is much lower than its adsorption free energy (61.5 vs. 292.8 kJ mol<sup>-1</sup>).

$C_2H_3$  is the common intermediate of three pathways studied, so identifying which pathway is the most favorable is of specific interest. Starting from  $C_2H_3 + H$  species (Figure 3), the overall activation free energies of three pathways are 72.0, 72.0, and 95.3 kJ mol<sup>-1</sup>, respectively, indicating that the  $CH_3CH$  intermediate pathway is unfavorable. However,  $C_2H_4$  prefers to desorb from the catalyst surface rather than being hydrogenated to  $C_2H_5$  (68.1 vs. 81.1 kJ mol<sup>-1</sup>), namely, the  $C_2H_4$  desorption pathway is the optimal pathway to form gaseous  $C_2H_4$ , and therefore the Cu(111) surface exhibits a better selectivity towards  $C_2H_4$  formation.

For the selective hydrogenation process of  $C_2H_2$ , besides  $C_2H_4$  over-hydrogenation to ethane, the high molecular weight oligomeric species such as oligomers from  $C_2H_2$  polymerization is the very important issue.<sup>[48]</sup> These oligomers and polymers are commonly referred to as  $C_{4+}$ , and the liquid part of  $C_{4+}$  is named "green oil",<sup>[49]</sup> moreover, previous studies<sup>[34,50,51]</sup> have proposed that 1,3-butadiene may be the precursor for green oil formation. Thus, the formation of 1,3-butadiene is examined. The hydrogenation–coupling pathway and coupling–hydrogenation pathway are used to investigate the formation of 1,3-butadiene.<sup>[52]</sup>

As shown in Figure S18 (in the Supporting Information), the  $C_2H_3 + C_2H_3$  pathway is the most favorable reaction pathway to form 1,3-butadiene on the Cu(111) surface, this pathway has the overall activation free energy of  $209.1 \text{ kJ mol}^{-1}$ , which is higher than that the formation of ethylene ( $121.6 \text{ kJ mol}^{-1}$ ), suggesting that the formation of  $C_2H_4$  is much easier than the formation of 1,3-butadiene over the Cu(111) surface. Moreover, when Pd is doped into Cu catalysts, it enhances the dissociation of  $H_2$ ,<sup>[3]</sup> which is more favorable for the hydrogenation of  $C_2H_2$ , and inhibits the coupling reaction to 1,3-butadiene, which means that Pd-doped Cu catalysts are more favorable for the formation of  $C_2H_4$  instead of the formation of 1,3-butadiene.

### 3.3.2. $C_2H_2$ hydrogenation on the Pd-doped Cu(111) surface

Similar to the Cu(111) surface, on  $Pd_9Cu_0$ ,  $Pd_6Cu_3$ ,  $Pd_3Cu_6$ , and  $Pd_1Cu_8$  surfaces, starting from  $C_2H_3 + H$  species (Figure S6 in the Supporting Information), the pathways via the  $C_2H_4$  intermediate are more favorable than that via the  $CHCH_3$  intermediate. Moreover,  $C_2H_4$  prefers desorption from the catalyst surface over its hydrogenation on  $Pd_6Cu_3$ ,  $Pd_3Cu_6$ , and  $Pd_1Cu_8$  surfaces, which exhibits a better selectivity towards  $C_2H_4$  formation. However, the  $Pd_9Cu_0$  surface more readily results in  $C_2H_2$  over-hydrogenation to ethane as  $C_2H_4$  prefers to be hydrogenated instead of desorbing. In addition, the  $Pd_9Cu_0$  surface with a Pd monolayer supported on Cu(111) has a similar catalytic performance with Pd catalysts; both exhibit a poor selectivity towards  $C_2H_4$  formation.<sup>[33,53–59]</sup>

As the number of doped Pd atoms over the Cu(111) surface increases, the activation free energy of  $C_2H_2$  hydrogenation decreases, suggesting that the catalytic activity of PdCu bimetallic catalyst in  $C_2H_2$  hydrogenation is enhanced, which agrees with the experimental facts that Pd catalyst exhibits a higher catalytic activity in  $C_2H_2$  hydrogenation.<sup>[19,33,50]</sup>

### 3.3.3. The selectivity towards $C_2H_4$ formation on Cu(111) and Pd-doped Cu(111) surfaces

As mentioned above, as the  $CH_3CH$  intermediate pathway is less likely to occur, it has little effect on the selectivity towards  $C_2H_4$  formation; as a result, both  $C_2H_4$  hydrogenation and its desorption determine the selectivity towards  $C_2H_4$  formation. In this study, aiming at quantitatively evaluating the selectivity towards  $C_2H_4$  formation over Cu-based catalysts, the difference between the activation free energy of  $C_2H_4$  hydrogenation and

the absolute value of  $C_2H_4$  adsorption free energy,  $\Delta G_a$ , is obtained according to Equation (1), which has been widely used.<sup>[33,60,61]</sup>

$$\Delta G_a = G_a - |G_{ads}| \quad (1)$$

Where  $G_a$  is the activation free energy of  $C_2H_4$  hydrogenation, and  $G_{ads}$  is the adsorption free energy of  $C_2H_4$ . The more positive  $\Delta G_a$  is, the better the selectivity towards  $C_2H_4$  formation is.

As listed in Table 2, according to the value of  $\Delta G_a$  ( $\text{kJ mol}^{-1}$ ), the selectivity towards  $C_2H_4$  formation follows the order  $Pd_1Cu_8$  ( $49.7$ ) >  $Pd_3Cu_6$  ( $34.1$ ) >  $Cu(111)$  ( $13.0$ ) >  $Pd_6Cu_3$  ( $8.1$ ) >  $Pd_9Cu_0$  ( $-3.0$ ), suggesting that when one or three Pd atoms as the monomer is doped into a Cu(111) surface,  $Pd_1Cu_8$  and  $Pd_3Cu_6$  surfaces present a better selectivity towards  $C_2H_4$  formation than a Cu(111) surface does. Whereas  $Pd_6Cu_3$  and  $Pd_9Cu_0$  surfaces exhibit poorer selectivity towards  $C_2H_4$  formation than a Cu(111) surface does, especially, the  $Pd_9Cu_0$  surface presents a similar selectivity with Pd catalysts; both have a good selectivity towards ethane instead of  $C_2H_4$ .

**Table 2.** Hydrogenation activation free energy ( $G_a$  in  $\text{kJ mol}^{-1}$ ) and the adsorption free energy ( $G_{ads}$  in  $\text{kJ mol}^{-1}$ ) of  $C_2H_4$ , the differences ( $\Delta G_a$  in  $\text{kJ mol}^{-1}$ ) between  $G_a$  and  $G_{ads}$ , as well as the reaction rate ( $r$  in  $\text{s}^{-1} \text{ site}^{-1}$ ) of  $C_2H_2$  hydrogenation to  $C_2H_4$  over different Pd-doped Cu surfaces at 425 K.

Surfaces	$G_a$	$G_{ads}$	$\Delta G_a$	$r$
Cu(111)	81.1	68.1	13.0	$1.00 \times 10^{-2}$
$Pd_1Cu_8$	139.2	89.5	49.7	$5.79 \times 10^1$
$Pd_3Cu_6$	120.2	86.1	34.1	$4.88 \times 10^1$
$Pd_6Cu_3$	87.9	79.8	8.1	$4.27 \times 10^3$
$Pd_9Cu_0$	89.8	92.8	-3.0	$5.01 \times 10^4$
$Pd_5Pd_{sub}Cu$	132.9	100.7	32.2	$1.06 \times 10^9$
$Pd_1Pd_{sub}Cu-I$	124.5	92.9	31.6	$3.85 \times 10^2$
$Pd_3Pd_{sub}Cu$	153.8	108.0	45.8	$9.78 \times 10^5$
$Pd_1Pd_{sub}Cu-II$	125.5	103.6	21.9	$4.93 \times 10^0$
$Pd_2Pd_{sub}Cu-II$	125.0	105.3	19.7	$5.07 \times 10^0$
$Pd_3Pd_{sub}Cu$	125.1	103.7	21.4	$9.73 \times 10^0$
$Pd_3Pd_{sub}Cu-I$	113.8	106.5	7.3	$6.30 \times 10^1$
$Pd_3Pd_{sub}Cu-II$	139.6	98.2	41.4	$2.57 \times 10^0$
$Pd_3Pd_{sub}Cu-III$	119.2	83.2	36.0	$7.00 \times 10^{-1}$
$Pd_6Pd_{sub}Cu$	145.7	115.4	30.3	$1.00 \times 10^1$
$Pd_{sub}Cu$	106.1	63.3	42.8	$3.94 \times 10^{-3}$

### 3.3.4. The activity of $C_2H_4$ formation

Aiming at quantitatively describing the catalytic activity of Pd-doped Cu catalysts in  $C_2H_2$  hydrogenation to  $C_2H_4$ , on the basis of the two-step model reported by Hu et al.<sup>[62,63]</sup> (see details in Part 2 of the Supporting Information), the reaction rate can be obtained, in which the coverage of adsorbed species in the selective hydrogenation of  $C_2H_2$  is considered.

The reaction rates ( $\text{s}^{-1} \text{ site}^{-1}$ ) of  $C_2H_2$  hydrogenation to  $C_2H_4$  (see Table 2) show that the catalytic activity follows the order:  $Pd_9Cu_0$  ( $5.01 \times 10^4$ ) >  $Pd_6Cu_3$  ( $4.27 \times 10^3$ ) >  $Pd_1Cu_8$  ( $5.79 \times 10^1$ ) >  $Pd_3Cu_6$  ( $4.88 \times 10^1$ ) >  $Cu(111)$  ( $1.00 \times 10^{-2}$ ), namely, with the increasing number of doped Pd atoms over a Cu(111) surface, the catalytic activity of a Pd-doped Cu(111) surface increases.

### 3.3.5. The ensemble effects of surface Pd atoms as active sites on the activity and selectivity

Projected density of states (pDOS) is calculated to deeply illustrate the effects of the surface Pd ensemble on the activity and selectivity of  $C_2H_4$  formation, the d-band center of  $Pd_1Cu_8$ ,  $Pd_3Cu_6$ ,  $Pd_6Cu_3$ , and  $Pd_9Cu_0$  surfaces is shown in Figure 4 (details in Figure S16 in the Supporting Information), the results show that as the number of doped Pd atoms increases, the catalytic activity of  $C_2H_4$  formation increases, accordingly, the d-band center is far from the Fermi energy level. According to the values of  $\Delta G_a$ , the selectivity towards  $C_2H_4$  formation decreases, which is attributed to the increasing catalytic activity in  $C_2H_4$  hydrogenation to  $C_2H_5$ , and therefore in ethane formation. In addition, the findings by Pallassana and Neurock<sup>[64]</sup> on  $C_2H_4$  hydrogenation suggest that the C–H bond activation of ethyl and ethylene is primarily guided by electron-back donation to the antibonding  $\sigma CH^*$  orbital, the catalytic activity of C–H bond formation increases on Pd catalyst surfaces where the d-band is far from the Fermi level. These also agree with the previous studies about  $CH_x$  hydrogenation to  $CH_4$ .<sup>[65–67]</sup>

The above results show that over Pd-doped Cu(111) surfaces, the higher the selectivity towards  $C_2H_4$  formation is, the lower the activity towards  $C_2H_4$  formation is. Moreover, compared with Cu(111), both  $Pd_1Cu_8$  and  $Pd_3Cu_6$  surfaces with only surface single-atom Pd monomer sites present a high selectivity and a relatively low activity in  $C_2H_4$  formation, whereas  $Pd_6Cu_3$ ,  $Pd_9Cu_0$ , and Pd(111) surfaces exhibit a low selectivity and a relatively high activity owing to the existence of surface Pd dimer and trimer sites. These results also mean that the Pd-Cu-Cu trimer ensemble over  $Pd_1Cu_8$  and  $Pd_3Cu_6$  surfaces is of benefit for the selectivity toward  $C_2H_4$  formation, and the Pd-Cu dimer ensemble is of benefit for the activity of  $C_2H_4$  formation. Our results agree with the theoretical and experimental studies by Feng et al.<sup>[68]</sup> that the (110) surface of  $Pm\bar{3}m$  PdIn with single-atom Pd sites shows high selectivity for  $C_2H_2$  hydro-

genation to  $C_2H_4$ , whereas the (111) surface of  $P4/mmm$  Pd<sub>3</sub>In with Pd trimer sites shows low selectivity. Thus, the catalytic activity and selectivity of  $C_2H_4$  formation over a Pd-doped Cu(111) surface markedly depend on the Pd geometrical distribution, namely, the surface Pd ensemble effect.<sup>[7,9]</sup>

Overall, for the surface ensemble, these surface ensemble models can also present the surface Pd segregation over the Cu(111) surface, a Pd-doped Cu(111) surface with the reduction of contiguous Pd sites as active sites is highly efficient in  $C_2H_2$  hydrogenation to  $C_2H_4$ , which can suppress ethane formation as a result of the surface Pd ensemble. Particularly, the  $Pd_1Cu_8$  surface with the single-atom Pd sites and the smallest surface Pd ensemble significantly enhances the selectivity towards  $C_2H_4$  formation. However, it is noted that the activity and selectivity in  $C_2H_2$  hydrogenation to  $C_2H_4$  cannot be tuned simultaneously by a surface Pd ensemble effect over a Cu(111) surface. In addition, the formation energy ( $\text{kJ mol}^{-1}$ )<sup>[69–71]</sup> (details in the Part 6 of the Supporting Information) shows that the stability of Pd-doped Cu(111) with different surface Pd ensembles follows the order:  $Pd_9Cu_0$  (10.9) <  $Pd_6Cu_3$  (–4.1) <  $Pd_3Cu_6$  (–20.9) <  $Pd_1Cu_8$  (–24.5), indicating that the formation of the  $Pd_1Cu_8$  surface is the most favorable, and it is the most stable among the four Pd-doped Cu(111) surfaces.

### 3.4. $C_2H_2$ hydrogenation on the sublayer Pd-doped $Pd_1Cu_8$ surface

As discussed above, the  $Pd_1Cu_8$  surface exhibits the highest selectivity towards  $C_2H_4$  formation; however, its catalytic activity is moderate. Moreover, it is difficult to simultaneously achieve high selectivity and activity by the Pd ensemble effect over Pd-doped Cu(111) surfaces. Fortunately, a previous study<sup>[3]</sup> clearly showed that the ensemble composed of the surface and contiguous sublayer Pd atoms over a Cu(111) surface as active sites can effectively enhance the catalytic activity of  $H_2$  dissociation.

In this section, based on the  $Pd_1Cu_8$  surface, we turn our attention to the ensemble composed of the surface and sublayer Pd atoms as active sites, and its effect on the activity and selectivity of  $C_2H_4$  formation. As shown in Figure 1, the sublayer Pd-doped  $Pd_1Cu_8$  surfaces with one, two, three, and six sublayer Cu atoms replaced by Pd atoms are examined, in which the surface and sublayer Pd atoms may be either joined together or unconnected to each other. Moreover, two differences exist between the ensemble of surface joint Pd atoms and that of one surface and its joint sublayer Pd atoms, one is the structure of the models, which represent different ensembles; the other is the electronic properties of the models, which change the catalytic activity and selectivity.

#### 3.4.1. One-sublayer Pd-doped $Pd_1Cu_8$ surface

For the one-sublayer Pd-doped  $Pd_1Cu_8$  surface, as shown in Figure 1(f) and (g), two types of surface models exist according to the connection pattern be-

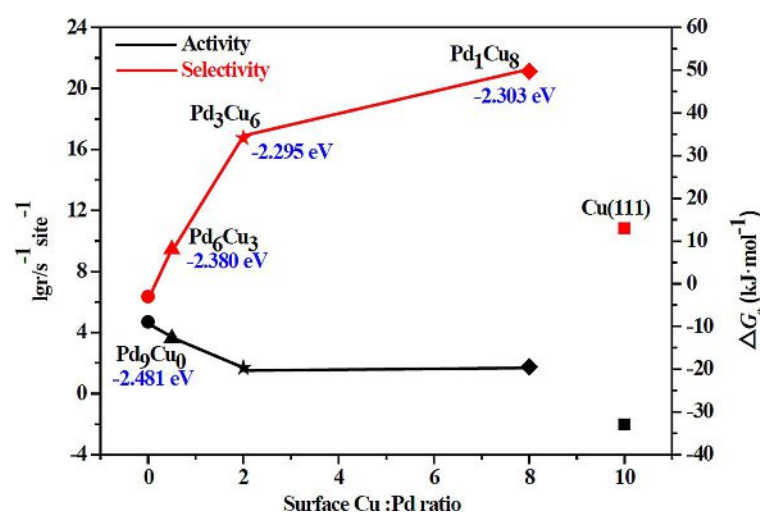


**Figure 4.** The relationship for the selectivity and the reaction rate of  $C_2H_2$  hydrogenation to  $C_2H_4$  as a function of surface Cu/Pd ratio over different Pd-doped Cu(111) surfaces, and the values of  $\lg r$  and  $\Delta G_a$  on the y axis are employed to represent the catalytic activity and selectivity of the catalyst, respectively.

tween the surface and sublayer Pd atoms, one is a Pd<sub>5</sub>Pd<sub>sub</sub>Cu surface with one surface Pd atom connecting only one sublayer Pd atom; the other is a Pd<sub>5</sub>Pd<sub>sub</sub>Cu-I surface where one surface Pd atom does not connect with only one sublayer Pd atom.

On Pd<sub>5</sub>Pd<sub>sub</sub>Cu and Pd<sub>5</sub>Pd<sub>sub</sub>Cu-I surfaces, the C<sub>2</sub>H<sub>4</sub> desorption pathway is favorable to form gaseous C<sub>2</sub>H<sub>4</sub> (Figure S8 in the Supporting Information). As listed in Table 2, the selectivity is towards C<sub>2</sub>H<sub>4</sub> formation with the ΔG<sub>a</sub> on Pd<sub>5</sub>Pd<sub>sub</sub>Cu and Pd<sub>5</sub>Pd<sub>sub</sub>Cu-I surfaces being 32.2 and 31.6 kJ mol<sup>-1</sup>. The activity of C<sub>2</sub>H<sub>4</sub> formation on the Pd<sub>5</sub>Pd<sub>sub</sub>Cu surface is much larger than that on the Pd<sub>5</sub>Pd<sub>sub</sub>Cu-I surface (1.06 × 10<sup>9</sup> vs. 3.85 × 10<sup>2</sup> s<sup>-1</sup> site<sup>-1</sup>). Thus, the Pd<sub>5</sub>Pd<sub>sub</sub>Cu surface exhibits a high activity and selectivity in C<sub>2</sub>H<sub>2</sub> hydrogenation to C<sub>2</sub>H<sub>4</sub>.

### 3.4.2. Two-sublayer Pd-doped Pd<sub>1</sub>Cu<sub>8</sub> surface

For the two-sublayer Pd-doped Pd<sub>1</sub>Cu<sub>8</sub> surface, as shown in Figure 1(h)–(j), three types of surface models exist: the Pd<sub>5</sub>2Pd<sub>sub</sub>Cu surface is that with one surface Pd atom connected with two sublayer Pd atoms; Pd<sub>5</sub>2Pd<sub>sub</sub>Cu-I surfaces have one surface Pd atom connected with only one sublayer Pd atom; the Pd<sub>5</sub>2Pd<sub>sub</sub>Cu-II surface is where one surface Pd atom does not connect with any sublayer Pd atoms.

The C<sub>2</sub>H<sub>4</sub> desorption pathway is still the favored pathway to form gaseous C<sub>2</sub>H<sub>4</sub> on these three surfaces (Figure S10 in the Supporting Information). As listed in Table 2, the ΔG<sub>a</sub> on the Pd<sub>5</sub>2Pd<sub>sub</sub>Cu surface is 45.8 kJ mol<sup>-1</sup>, which is higher than those on Pd<sub>5</sub>2Pd<sub>sub</sub>Cu-I and Pd<sub>5</sub>2Pd<sub>sub</sub>Cu-II surfaces (21.9 and 19.7 kJ mol<sup>-1</sup>). The reaction rate on the Pd<sub>5</sub>2Pd<sub>sub</sub>Cu surface (9.78 × 10<sup>5</sup> s<sup>-1</sup> site<sup>-1</sup>) is much larger than those on Pd<sub>5</sub>2Pd<sub>sub</sub>Cu-I and Pd<sub>5</sub>2Pd<sub>sub</sub>Cu-II surfaces (4.93 × 10<sup>0</sup> and 5.07 × 10<sup>0</sup> s<sup>-1</sup> site<sup>-1</sup>). Thus, the Pd<sub>5</sub>2Pd<sub>sub</sub>Cu surface exhibits a high activity and selectivity towards C<sub>2</sub>H<sub>4</sub> formation.

### 3.4.3. Three-sublayer Pd-doped Pd<sub>1</sub>Cu<sub>8</sub> surfaces

As shown in Figure 1(k)–(n), four types of surface models are considered, Pd<sub>5</sub>3Pd<sub>sub</sub>Cu, Pd<sub>5</sub>3Pd<sub>sub</sub>Cu-I, and Pd<sub>5</sub>3Pd<sub>sub</sub>Cu-II surfaces, where one surface Pd atom is connected with three, two, and one sublayer Pd atoms, respectively. The Pd<sub>5</sub>3Pd<sub>sub</sub>Cu-III surface is where one surface Pd atom does not connect with any sublayer Pd atom.

The C<sub>2</sub>H<sub>4</sub> desorption pathway is still the favorable pathway to form gaseous C<sub>2</sub>H<sub>4</sub> on these surfaces (Figure S12 in the Supporting Information). As listed in Table 2, the ΔG<sub>a</sub> (kJ mol<sup>-1</sup>) follows the order Pd<sub>5</sub>3Pd<sub>sub</sub>Cu-II (41.4) > Pd<sub>5</sub>3Pd<sub>sub</sub>Cu-III (36.0) > Pd<sub>5</sub>3Pd<sub>sub</sub>Cu (21.4) > Pd<sub>5</sub>3Pd<sub>sub</sub>Cu-I (7.3). The reaction rates on Pd<sub>5</sub>3Pd<sub>sub</sub>Cu, Pd<sub>5</sub>3Pd<sub>sub</sub>Cu-I, Pd<sub>5</sub>3Pd<sub>sub</sub>Cu-II, and Pd<sub>5</sub>3Pd<sub>sub</sub>Cu-III surfaces are competitive, with the corresponding values of 9.73 × 10<sup>0</sup>, 6.30 × 10<sup>1</sup>, 2.57 × 10<sup>0</sup>, and 7.00 × 10<sup>-1</sup> s<sup>-1</sup> site<sup>-1</sup>, respectively. Thus, taking the activity and selectivity into consideration, the Pd<sub>5</sub>3Pd<sub>sub</sub>Cu-II surface exhibits a better catalytic performance towards C<sub>2</sub>H<sub>4</sub> formation.

### 3.4.4. Six-sublayer Pd-doped Pd<sub>1</sub>Cu<sub>8</sub> surfaces

Aiming at examining the effect of the number of sublayer Pd atoms on the catalytic performance of C<sub>2</sub>H<sub>4</sub> formation, a six-sublayer Pd-doped Pd<sub>1</sub>Cu<sub>8</sub> surface with one surface Pd atom connecting three sublayer Pd atoms, Pd<sub>5</sub>6Pd<sub>sub</sub>Cu surface, is considered (Figure 1(o)). The results show that the C<sub>2</sub>H<sub>4</sub> desorption pathway is more favorable than the other two pathways (Figure S14(a) in the Supporting Information). Both ΔG<sub>a</sub> and the reaction rate are 30.3 kJ mol<sup>-1</sup> and 1.00 × 10<sup>1</sup> s<sup>-1</sup> site<sup>-1</sup>, respectively.

### 3.4.5. The ensemble effect composed of surface and sublayer Pd atoms as active sites on the activity and selectivity in C<sub>2</sub>H<sub>4</sub> formation

As discussed above, for one-, two-, three-, and six-sublayer Pd-doped Pd<sub>1</sub>Cu<sub>8</sub> surfaces, there is good selectivity towards C<sub>2</sub>H<sub>4</sub> formation with the ΔG<sub>a</sub> values of 32.2, 45.8, 41.4, and 30.3 kJ mol<sup>-1</sup>, respectively. Pd<sub>5</sub>Pd<sub>sub</sub>Cu, Pd<sub>5</sub>2Pd<sub>sub</sub>Cu, Pd<sub>5</sub>3Pd<sub>sub</sub>Cu-II, and Pd<sub>5</sub>6Pd<sub>sub</sub>Cu surfaces exhibit high activity for C<sub>2</sub>H<sub>4</sub> formation, the reaction rates are 1.06 × 10<sup>9</sup>, 9.78 × 10<sup>5</sup>, 2.57 × 10<sup>0</sup>, and 1.00 × 10<sup>1</sup> s<sup>-1</sup> site<sup>-1</sup>, respectively. The ΔG<sub>a</sub> and *r* on the Pd<sub>1</sub>Cu<sub>8</sub> surface are 49.7 kJ mol<sup>-1</sup> and 5.79 × 10<sup>1</sup> s<sup>-1</sup> site<sup>-1</sup>.

As shown in Figure 5, as the number of sublayer Pd atoms increases, the d-band center (details in Figure S17 in the Supporting Information) approaches the Fermi level, and the catalytic activity decreases. The selectivity towards C<sub>2</sub>H<sub>4</sub> formation presents a volcanic curve; the highest selectivity appears on the Pd<sub>5</sub>2Pd<sub>sub</sub>Cu surface, which is close to that on the Pd<sub>1</sub>Cu<sub>8</sub> surface. Clearly, compared with the Pd<sub>1</sub>Cu<sub>8</sub> surface, both Pd<sub>5</sub>Pd<sub>sub</sub>Cu and Pd<sub>5</sub>2Pd<sub>sub</sub>Cu surfaces significantly enhance the catalytic activity of C<sub>2</sub>H<sub>4</sub> formation, whereas Pd<sub>5</sub>3Pd<sub>sub</sub>Cu-II and Pd<sub>5</sub>6Pd<sub>sub</sub>Cu surfaces do not improve the catalytic activity of C<sub>2</sub>H<sub>4</sub> formation. Thus, the catalytic activity of sublayer Pd-doped Pd<sub>1</sub>Cu<sub>8</sub> surfaces in C<sub>2</sub>H<sub>4</sub> formation markedly depends

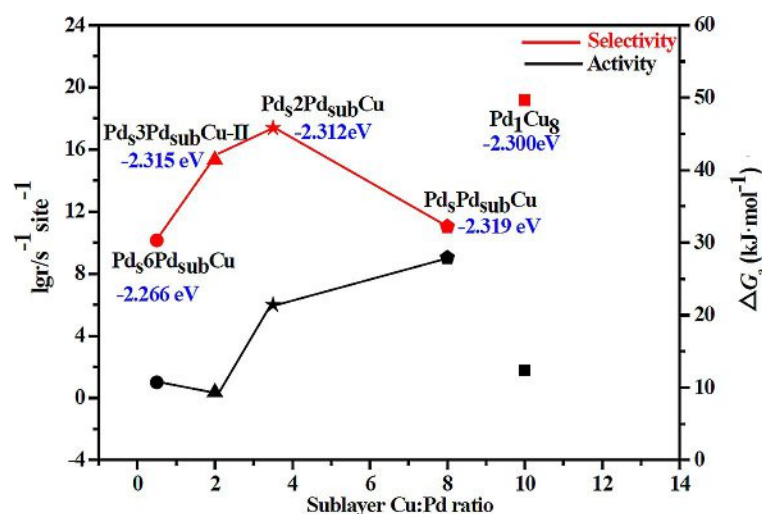


**Figure 5.** The relationship between the selectivity and the reaction rate of C<sub>2</sub>H<sub>2</sub> hydrogenation to C<sub>2</sub>H<sub>4</sub> as a function of the surface Cu/Pd ratio over different Pd-doped Pd<sub>1</sub>Cu<sub>8</sub> surfaces, and the values of *lgr* and ΔG<sub>a</sub> on the y axis are employed to represent the catalytic activity and selectivity of the catalyst, respectively.

on the number of sublayer Pd atoms,  $n$ . Only when  $n \leq 2$  do both  $\text{Pd}_3\text{Pd}_{\text{sub}}\text{Cu}$  and  $\text{Pd}_52\text{Pd}_{\text{sub}}\text{Cu}$  surfaces with the joint surface–sublayer Pd ensembles exhibit an excellent catalytic activity for  $\text{C}_2\text{H}_4$  formation, suggesting that only the joint surface–sublayer Pd ensembles play a role as the active sites in  $\text{C}_2\text{H}_2$  hydrogenation to  $\text{C}_2\text{H}_4$ , namely, the catalytic activity depends on the ensemble arrangement.

### 3.5. General discussions

These calculations elucidate the activity and selectivity of  $\text{C}_2\text{H}_2$  hydrogenation to  $\text{C}_2\text{H}_4$  on Pd-doped Cu surfaces with a particular focus on the ensemble of surface Pd atoms and the ensemble composed of surface and sublayer Pd atoms. The ensemble of surface Pd atoms is an effective way to tune the selectivity towards  $\text{C}_2\text{H}_4$  formation. The  $\text{Pd}_1\text{Cu}_8$  surface with the smallest surface Pd ensemble as active sites exhibits the highest selectivity towards  $\text{C}_2\text{H}_4$  formation ( $\Delta G_a = 49.7 \text{ kJ mol}^{-1}$ ). On the other hand, the activity of the  $\text{Pd}_1\text{Cu}_8$  surface is still relatively low ( $r = 5.79 \times 10^1 \text{ s}^{-1} \text{ site}^{-1}$ ) compared with the Cu(111) surface ( $\Delta G_a = 13.0 \text{ kJ mol}^{-1}$ ,  $r = 1.00 \times 10^{-2} \text{ s}^{-1} \text{ site}^{-1}$ ); one isolated Pd atom doped into the sublayer of a Cu(111) surface ( $\text{Pd}_{\text{sub}}\text{Cu}$  surface) was examined (see Figure S14(b) in the Supporting Information), suggesting that the  $\text{C}_2\text{H}_4$  desorption pathway is more favorable than other two pathways: the  $\Delta G_a$  towards  $\text{C}_2\text{H}_4$  formation is  $42.8 \text{ kJ mol}^{-1}$ , the reaction rate is  $3.94 \times 10^{-3} \text{ s}^{-1} \text{ site}^{-1}$ . However, compared with the reaction rate on the Cu(111) surface ( $1.00 \times 10^{-2} \text{ s}^{-1} \text{ site}^{-1}$ ), the  $\text{Pd}_{\text{sub}}\text{Cu}$  surface is much less reactive, which is similar to the  $\text{Pd}_1\text{Cu}_8$  surface. Thus, one isolated Pd atom on a surface or sublayer of Cu(111) does not contribute to the high catalytic activity.

The ensemble composed of one surface Pd atom and its joint sublayer Pd atoms is an effective way to tune the catalytic activity for  $\text{C}_2\text{H}_4$  formation. A very small quantity of Pd doped into the surface and sublayer and joined together exhibits strong catalytic activity ( $r = 1.06 \times 10^9$  and  $9.78 \times 10^5 \text{ s}^{-1} \text{ site}^{-1}$  for  $\text{Pd}_3\text{Pd}_{\text{sub}}\text{Cu}$  and  $\text{Pd}_52\text{Pd}_{\text{sub}}\text{Cu}$ ). Moreover, the  $\text{Pd}_1\text{Cu}_8$  surface with the smallest surface Pd ensemble as active sites still keeps a relatively good selectivity towards  $\text{C}_2\text{H}_4$  formation ( $\Delta G_a = 32.2$  and  $45.8 \text{ kJ mol}^{-1}$ ), which is close to the selectivity of  $\text{C}_2\text{H}_4$  formation on the single  $\text{Pd}_1\text{Cu}_8$  surface ( $\Delta G_a = 49.7 \text{ kJ mol}^{-1}$ ).

For Pd-doped Cu bimetallic catalysts, the higher catalytic activity corresponds to the lower surface d-band center of the bimetallic catalyst. As the d-band center can be more efficiently obtained than the reaction rate, the surface d-band center of Pd-doped Cu bimetallic catalysts can be used as a good “descriptor” for the corresponding catalytic activity of  $\text{C}_2\text{H}_4$  formation. This is quite useful for rapid screening of catalytic activity in the design of improved catalysts, including Pd-doped Cu bimetallic catalysts and other precious metal-doped common metal bimetallic catalysts.

Therefore, only the ensemble composed of a surface and joint sublayer Pd atoms over a Pd-doped Cu surface is responsible for the enhanced catalytic activity and selectivity in  $\text{C}_2\text{H}_2$  hydrogenation to  $\text{C}_2\text{H}_4$ , which can be experimentally realized by a Cu catalyst doped with a very small quantity of Pd into the surface and sublayer to join together. It has been also ex-

perimentally confirmed that a small quantity of Pd atoms incorporated into the surface and sublayer of Cu(111) can be developed.<sup>[3,14,16,17]</sup> Our results not only give guidance for improving the catalytic performances of Cu-Pd alloy systems, but also provide an effective method for the design of other precious-metal-doped common metal catalysts in industrially key hydrogenation reactions.

### 4. Conclusions

Extensive DFT calculations have been used to elucidate the activity and selectivity for the selective hydrogenation of  $\text{C}_2\text{H}_2$  over Pd-doped Cu catalysts with different ensemble effects, identifying the specific active sites. For almost all Pd-doped Cu surface–sublayer configurations, the  $\text{C}_2\text{H}_4$  desorption pathway is the most favorable for gaseous  $\text{C}_2\text{H}_4$  formation. The catalytic activity of  $\text{C}_2\text{H}_2$  hydrogenation to  $\text{C}_2\text{H}_4$  increases with increasing Pd/Cu ratios on the surface or in the sublayer, and the surface reactivity increases, the further the d-band center of a Pd-doped Cu surface is from the Fermi energy level. The surface Pd ensemble is more sensitive to the selectivity, and the sublayer Pd ensemble is more sensitive to the activity in  $\text{C}_2\text{H}_2$  hydrogenation to  $\text{C}_2\text{H}_4$ . The ensemble composed of a surface and joint sublayer Pd atoms over a Pd-doped Cu surface contributes to the enhanced catalytic activity and selectivity in  $\text{C}_2\text{H}_2$  hydrogenation to  $\text{C}_2\text{H}_4$ , which can be experimentally realized by a Cu catalyst doped with a very small quantity of Pd into the surface and sublayer to join together.

This detailed understanding for the mechanisms of enhanced activity and selectivity in  $\text{C}_2\text{H}_2$  hydrogenation to  $\text{C}_2\text{H}_4$  shows that the performance of Pd-doped Cu catalysts can be tuned by controlling the doped Pd atom ensemble effects, which can provide an effective method for the design of bimetallic catalysts with the precious-metal-doped common metal motif for industrially key hydrogenation reactions.

### Acknowledgments

This work was financially supported by the National Natural Science Foundation of China (No. 21776193, 21476155), the Key Projects of the National Natural Science Foundation of China (21736007), the China Scholarship Council (201606935026), the Program for the Top Young Academic Leaders of Higher Learning Institutions of Shanxi, the Top Young Innovative Talents of Shanxi, and US NSF-sponsored NCAR-Wyoming Supercomputing Center (NWSC).

### Conflict of interest

The authors declare no conflict of interest.

**Keywords:** acetylene hydrogenation • activity • Cu-based catalyst • ensemble effect • selectivity

[1] A. J. McCue, A. M. Shepherd, J. A. Anderson, *Catal. Sci. Technol.* **2015**, *5*, 2880–2890.

- [2] J. W. A. Sachtler, G. A. Somorjai, *J. Catal.* **1983**, *81*, 77–94.
- [3] Q. Fu, Y. Luo, *ACS Catal.* **2013**, *3*, 1245–1252.
- [4] U. Schneider, H. Busse, R. Link, G. R. Castro, K. Wandelt, *J. Vac. Sci. Technol. A* **1994**, *12*, 2069–2073.
- [5] N. Kristian, Y. S. Yan, X. Wang, *Chem. Commun.* **2008**, 353–355.
- [6] M. Neurock, M. Janik, A. Wieckowski, *Faraday Discuss.* **2009**, *140*, 363–378.
- [7] D. W. Yuan, X. G. Gong, R. W. Wu, *J. Chem. Phys.* **2008**, *128*, 064706.
- [8] T. Duan, R. G. Zhang, L. X. Ling, B. J. Wang, *J. Phys. Chem. C* **2016**, *120*, 2234–2246.
- [9] D. W. Yuan, Z. R. Liu, *J. Power Sources* **2013**, *224*, 241–249.
- [10] J. W. Hong, D. Kim, Y. W. Lee, M. Kim, S. W. Kang, S. W. Han, *Angew. Chem. Int. Ed.* **2011**, *50*, 8876–8880; *Angew. Chem.* **2011**, *123*, 9038–9042.
- [11] D. H. Mei, P. A. Sheth, M. Neurock, C. M. Smith, *J. Catal.* **2006**, *242*, 1–15.
- [12] B. Bridier, N. López, J. Pérez-Ramírez, *J. Catal.* **2010**, *269*, 80–92.
- [13] B. Bridier, M. A. G. Hevia, N. López, J. Pérez-Ramírez, *J. Catal.* **2011**, *278*, 167–172.
- [14] G. Kyriakou, M. B. Boucher, A. D. Jewell, E. A. Lewis, T. J. Lawton, A. E. Baber, H. L. Tierney, M. Flytzani-Stephanopoulos, E. C. H. Sykes, *Science* **2012**, *335*, 1209–1212.
- [15] A. J. McCue, C. J. McRitchie, A. M. Shepherd, J. A. Anderson, *J. Catal.* **2014**, *319*, 127–135.
- [16] H. L. Tierney, A. E. Baber, J. R. Kitchin, E. C. H. Sykes, *Phys. Rev. Lett.* **2009**, *103*, 246102.
- [17] A. Bach Aena, E. Laegsgaard, A. V. Ruban, I. Stensgaard, *Surf. Sci.* **1998**, *408*, 43–56.
- [18] M. Neurock, *J. Catal.* **2003**, *216*, 73–88.
- [19] F. Studt, F. Abild-Pedersen, T. Bligaard, R. Z. Sorensen, C. H. Christensen, J. K. Nørskov, *Science* **2008**, *320*, 1320–1322.
- [20] J. K. Nørskov, T. Bligaard, B. Hvolbaek, F. Abild-Pedersen, I. Chorkendorff, C. H. Christensen, *Chem. Soc. Rev.* **2008**, *37*, 2163–2171.
- [21] S. Kattel, P. J. Ramírez, J. G. Chen, J. A. Rodriguez, P. Liu, *Science* **2017**, *355*, 1296–1299.
- [22] P. Zhai, C. Xu, R. Gao, X. Liu, M. Li, W. Li, X. Fu, C. Jia, J. Xie, M. Zhao, X. Wang, Y. Li, Q. Zhang, X. Wen, D. Ma, *Angew. Chem. Int. Ed.* **2016**, *55*, 9902–9907; *Angew. Chem.* **2016**, *128*, 10056–10061.
- [23] T. V. Cleve, S. Moniri, G. Belok, K. L. More, S. Linic, *ACS Catal.* **2017**, *7*, 17–24.
- [24] E. M. Gallego, M. T. Portilla, C. Paris, A. León-Escamilla, M. Boronat, M. Moliner, A. Corma, *Science* **2017**, *355*, 1051–1054.
- [25] F. Göltl, C. Michel, P. C. Andrikopoulos, A. M. Love, J. Hafner, I. Hermans, P. Sautet, *ACS Catal.* **2016**, *6*, 8404–8409.
- [26] J. K. Nørskov, T. Bligaard, J. Rossmeisl, C. H. Christensen, *Nat. Chem.* **2009**, *1*, 37–46.
- [27] B. Delley, *J. Chem. Phys.* **2000**, *113*, 7756–7764.
- [28] B. Delley, *J. Chem. Phys.* **1990**, *92*, 508–517.
- [29] D. X. Tian, H. L. Zhang, J. J. Zhao, *Solid State Commun.* **2007**, *144*, 174–179.
- [30] C. G. Zhou, J. P. Wu, A. Nie, R. C. Forrey, A. Tachibana, H. S. Cheng, *J. Phys. Chem. C* **2007**, *111*, 12773–12778.
- [31] T. A. Halgren, W. N. Lipscomb, *Chem. Phys. Lett.* **1977**, *49*, 225–232.
- [32] N. Govind, M. Petersen, G. Fitzgerald, D. King-Smith, J. Andzelm, *Comput. Mater. Sci.* **2003**, *28*, 250–258.
- [33] B. Yang, R. Burch, C. Hardacre, G. Headdock, P. Hu, *J. Catal.* **2013**, *305*, 264–276.
- [34] D. Teschner, J. Borsodi, A. Wootsch, Z. Révay, M. Hävecker, A. Knop-Gericke, S. D. Jackson, R. Schlögl, *Science* **2008**, *320*, 86–89.
- [35] F. Studt, F. Abild-Pedersen, T. Bligaard, R. Z. Sørensen, C. H. Christensen, J. K. Nørskov, *Angew. Chem. Int. Ed.* **2008**, *47*, 9299–9302; *Angew. Chem.* **2008**, *120*, 9439–9442.
- [36] K. M. Neyman, S. Schauerer, *Angew. Chem. Int. Ed.* **2010**, *49*, 4743–4746; *Angew. Chem.* **2010**, *122*, 4851–4854.
- [37] M. García-Mota, B. Bridier, J. Pérez-Ramírez, N. López, *J. Catal.* **2010**, *273*, 92–102.
- [38] J. Galipaud, M. H. Martin, L. Roué, D. Guay, *J. Phys. Chem. C* **2013**, *117*, 2688–2698.
- [39] M. Friedrich, S. A. Villaseca, L. Szentmiklósi, D. Teschner, M. Armbruster, *Materials* **2013**, *6*, 2958–2977.
- [40] B. Yang, R. Burch, C. Hardacre, P. Hu, P. Hughes, *J. Phys. Chem. C* **2014**, *118*, 1560–1567.
- [41] B. Eren, D. Zherebetsky, L. L. Patera, C. H. Wu, H. Bluhm, C. Africh, L. W. Wang, G. A. Somorjai, M. Salmeron, *Science* **2016**, *351*, 475–478.
- [42] M. H. Zhang, R. Yao, H. X. Jiang, G. M. Li, Y. F. Chen, *Appl. Surf. Sci.* **2017**, *412*, 342–349.
- [43] X. C. Sun, R. G. Zhang, B. J. Wang, *Appl. Surf. Sci.* **2013**, *265*, 720–730.
- [44] W. Liu, J. S. Lian, Q. Jiang, *J. Phys. Chem. C* **2007**, *111*, 18189–18194.
- [45] B. Yang, R. Burch, C. Hardacre, G. Headdock, P. Hu, *ACS Catal.* **2012**, *2*, 1027–1032.
- [46] B. Li, X. L. Cui, D. Oui, D. M. Wen, M. D. Jiang, R. Krishna, H. Wu, R. B. Lin, Y. S. Chen, D. Q. Yuan, H. B. Xing, W. Zhou, Q. L. Ren, G. D. Qian, M. J. Zaworotko, B. L. Chen, *Adv. Mater.* **2017**, *29*, 1704210.
- [47] X. L. Cui, K. J. Chen, H. B. Xing, Q. W. Yang, R. Krishna, Z. B. Bao, H. Wu, W. Zhou, X. L. Dong, Y. Han, B. Li, Q. L. Ren, M. J. Zaworotko, B. L. Chen, *Science* **2016**, *353*, 141–144.
- [48] M. Wilde, K. Fukutani, W. Ludwig, B. Brandt, J. H. Fischer, S. Schauerer, H. J. Freund, *Angew. Chem. Int. Ed.* **2008**, *47*, 9289–9293; *Angew. Chem.* **2008**, *120*, 9430–9434.
- [49] A. N. R. Bos, K. R. Westerterp, *Chem. Eng. Process.* **1993**, *32*, 1–7.
- [50] S. Asplund, *J. Catal.* **1996**, *158*, 267–278.
- [51] M. Larsson, J. Jansson, S. Asplund, *J. Catal.* **1996**, *162*, 365–367.
- [52] M. Larsson, J. Jansson, S. Asplund, *J. Catal.* **1998**, *178*, 49–57.
- [53] F. M. McKenna, J. A. Anderson, *J. Catal.* **2011**, *281*, 231–240.
- [54] A. J. McCue, F. M. McKenna, J. A. Anderson, *Catal. Sci. Technol.* **2015**, *5*, 2449–2459.
- [55] B. Bridier, N. López, J. Pérez-Ramírez, *Dalton Trans.* **2010**, *39*, 8412–8419.
- [56] M. Armbruster, M. Behrens, F. Cinquini, K. Föttinger, Y. Grin, A. Haghofer, B. Klötzer, A. Knop-Gericke, H. Lorenz, A. Ota, S. Penner, J. Prinz, C. Rameshan, Z. Révay, D. Rosenthal, G. Rupprechter, D. Teschner, D. Torres, R. Wagner, R. Widmer, G. Wowsnick, *ChemCatChem* **2012**, *4*, 1048–1063.
- [57] S. Schauerer, N. Nilius, S. Shaikhtudinov, H. J. Freund, *Acc. Chem. Res.* **2013**, *46*, 1673–1681.
- [58] W. Ludwig, A. Savara, K. H. Dosert, S. Schauerer, *J. Catal.* **2011**, *284*, 148–156.
- [59] W. Ludwig, A. Savara, R. J. Madix, S. Schauerer, H. J. Freund, *J. Phys. Chem. C* **2012**, *116*, 3539–3544.
- [60] P. A. Sheth, M. Neurock, C. M. Smith, *J. Phys. Chem. B* **2003**, *107*, 792–801.
- [61] P. A. Sheth, M. Neurock, C. M. Smith, *J. Phys. Chem. B* **2005**, *109*, 12449–12466.
- [62] J. Cheng, P. Hu, *Angew. Chem. Int. Ed.* **2011**, *50*, 7650–7654; *Angew. Chem.* **2011**, *123*, 7792–7796.
- [63] J. Cheng, P. Hu, P. Ellis, S. French, G. Kelly, C. M. Lok, *J. Phys. Chem. C* **2008**, *112*, 1308–1311.
- [64] V. Pallassana, M. Neurock, *J. Catal.* **2000**, *191*, 301–317.
- [65] C. F. Huo, Y. W. Li, J. G. Wang, H. J. Jiao, *J. Am. Chem. Soc.* **2009**, *131*, 14713–14721.
- [66] T. H. Pham, Y. Y. Qi, J. Yang, X. Z. Duan, G. Qian, X. G. Zhou, D. Chen, W. K. Yuan, *ACS Catal.* **2015**, *5*, 2203–2208.
- [67] J. D. Li, E. Croiset, R. S. Luis, *J. Mol. Catal. A* **2012**, *365*, 103–114.
- [68] Q. C. Feng, S. Zhao, Y. Wang, J. C. Dong, W. X. Chen, D. S. He, D. S. Wang, J. Yang, Y. M. Zhu, H. L. Zhu, L. Gu, Z. Li, Y. X. Liu, R. Yu, J. Li, Y. D. Li, *J. Am. Chem. Soc.* **2017**, *139*, 7294–7301.
- [69] J. Li, H. Y. Zheng, X. C. Zhang, Z. Li, *Comput. Mater. Sci.* **2015**, *96*, 1–9.
- [70] H. K. Kim, J. W. Yang, S. B. Jo, B. Kang, S. K. Lee, H. Bong, G. Lee, K. S. Kim, K. Cho, *ACS Nano* **2013**, *7*, 1155–1162.
- [71] C. Di Valentin, G. Pacchioni, A. Selloni, *Chem. Mater.* **2005**, *17*, 6656–6665.

Manuscript received: November 29, 2017

Revised manuscript received: February 3, 2018

Accepted manuscript online: February 6, 2018

Version of record online: April 27, 2018